Lens Distortion for Close-Range Photogrammetry

*John G. Fryer** and *Duane C. Brown*
Geodetic Services, Inc., Melbourne, FL 32901

ABSTRACT: A brief review of the formulas for radial and decentering lens distortion is presented, with emphasis on the currently accepted representation of the decentering distortion. Recent technological advances, which include the large format close range camera, CRC-1, and the automated precision mono-comparator, AutoSet, caused the authors to reinvestigate the analytical plumb-line method of lens calibration. With AutoSet, measurements of 1000 images of points on plumb-lines are performed in under one hour and RMS plate residuals of one micrometre or less are produced. Brown's (1972) extension of Magill's formula for the variation of radial distortion with focusing is experimentally reverified with data of much higher precision than in previous investigations. The quality of the data allowed a more sensitive examination of the formula for decentering distortion, which led to the finding that decentering distortion also varies with focusing. A reinvestigation of the theory of decentering distortion extends the 1966 formulation by Brown to account for the variation experimentally observed. It is shown that decentering coefficients P_1 and P_2 for the lens focused at infinity need merely be appropriately rescaled in order to apply finite focusing. Implications of this discovery for close-range photogrammetry are explored.

INTRODUCTION—HISTORICAL REVIEW

THE THEORY AND FORMULATION of radial and decentering lens distortions adopted for use by the photogrammetric community in the last two decades can be traced to papers by Brown (1966, 1971, 1972). The first paper demonstrated the projective equivalence of the then widely accepted thin prism model for decentering distortion with the more rigorous and apparently contradictory formulation of Conrady (1919). In Conrady's model the radial component of decentering distortion is three times as large as for the thin prism model. However, an appropriate tilt of the camera axis accompanied by a shift in the principal point effectively compensates for the deficiency of the thin prism model. Because the accuracy of Conrady's model does not depend on compensative alteration of projective parameters, it has displaced the thin prism model as the generally accepted model for decentering distortion.

According to Conrady's model, the radial and tangential components of decentering distortion, Δr and Δt, of an image with coordinates x, y (referred to the principal point as origin) may be represented by the expressions

$$\begin{aligned} \Delta r &= 3\,P(r)\sin(\phi - \phi_0) \\ \Delta t &= P(r)\cos(\phi - \phi_0) \end{aligned} \tag{1}$$

in which ϕ is the angle between the positive x axis and the radius vector to the image point and r is the radial distance. The parameters of decentering distortion are defined by the phase angle ϕ_0, which represents the angle between the x axis and the axis of maximum tangential distortion, and by the profile function $P(r)$, which is in the form

$$P(r) = J_1 r^2 + J_2 r^4 + \ldots \tag{2}$$

where J_1, J_2 are the coefficients of the profile function. In terms of x, y components (Δx, Δy), Equations 1 are equivalent to

$$\Delta x = [P_1(r^2+2x^2)+2P_2xy][1+P_3r^2+\ldots] \tag{3}$$

$$\Delta y = [P_2(r^2+2y^2)+2P_1xy][1+P_3r^2+\ldots]$$

in which the new parameters P_1, P_2, P_3 are related to J_1, J_2, ϕ_0 by the expressions

$$\begin{aligned} P_1 &= -J_1\sin\phi_0 \\ P_2 &= J_1\cos\phi_0 \\ P_3 &= \frac{J_2}{J_1} \\ J_1 &= (P_1^2 + P_2^2)^{1/2} \\ J_2 &= J_1P_3 \\ \tan\phi_0 &= -\frac{P_1}{P_2} \end{aligned} \tag{4}$$

* On sabbatical leave from the Department of Civil Engineering and Surveying, University of Newcastle, New South Wales 2308, Australia.

PHOTOGRAMMETRIC ENGINEERING AND REMOTE SENSING,
Vol. 52, No. 1, January 1986, pp. 51–58.

0099-1112/86/5201-0051$02.25/0

Higher order terms (J_2, P_3, . . .) are rarely significant. As a result, Equations 3 reduce in practice to linear functions of P_1 and P_2.

As it stands, the above model for decentering distortion applies for the lens focused at infinity. It will be shown in due course that a simple modification will extend its applicability to focusing at finite distances.

In Brown (1971, 1972) it is shown that, for the highest accuracies in close-range photogrammetry, it is necessary to account for variation of radial lens distortion within the photographic field. The radial lens distortion profile for a lens focused at a distance s is of the form

$$dr_s = K_{1s}\, r^3 + K_{2s}\, r^5 + K_{3s}\, r^7 + \ldots \qquad (5)$$

and the corrections δx, δy to the image coordinates x, y for points in the focused plane are

$$\delta x = \frac{x}{r} dr_s$$
$$\delta y = \frac{y}{r} dr_s \qquad (6)$$

The precise dependence of the coefficients K_{1s}, K_{2s}, . . . on s is developed in the above references, as are further modifications appropriate for points not lying within the plane of focus.

The analytical plumb-line method (Brown, 1971) was developed as a rapid, practical way of computing lens distortion parameters at a range of magnifications from approximately 1:5 to 1:20. The principle of this technique lies in the truism that straight lines in object space should project through a perfect lens as straight line images. Any variation from straightness is attributed to radial or decentering distortion, and a least-squares adjustment is performed to determine the distortion parameters K_1, K_2, K_3, P_1, and P_2.

It should be appreciated that results of such a lens calibration can be contaminated in practice by uncorrected systematic errors in the comparator, by unflatness of the photographic surface, or by uncompensated deformations of film. Such sources of error must be adequately controlled or corrected if nonlinearity in measured images of plumb-lines is to be fully attributed to the lens.

Calibrations of radial distortion performed in the late 1960s typically had one-sigma values of about 2 micrometres, with root-mean-square (RMS) values of plate residuals being of similar magnitude. This level of precision was sufficient to illustrate the variation of radial distortion within the field of view and to confirm the validity of the model accounting for variation of radial distortion with camera focusing. The plumb-line calibrations also produced values for P_1 and P_2 that allowed J_1 and the tangential distortion profile to be calculated. The $J_1\, r^2$ profile had a standard error of about 2 micrometres at the maximum observed radial distance of 75 mm. Insufficient evidence could be obtained to draw firm conclusions concerning the precise behavior of decentering distortion with varying object distances.

ANALYTICAL PLUMB-LINE CALIBRATIONS IN THE MID-1980s

Some 15 years after the initial plumb-line calibrations reported in Brown (1971), several advances in technology induced the authors to reconsider the plumb-line method as an alternative or supplement to the (now) usual process of self-calibration for determining lens distortion. These technological improvements include the following:

- The large format 23 by 23-cm microprocessor-controlled close-range camera CRC-1 developed by Geodetic Services Inc. (Brown, 1984). This camera has a vacuum platen flat to within 2 or 3 micrometres (and calibrated to 0.25 μm). It also incorporates a set of 25 back-projected reseau targets that allow rigorous compensation for film deformation.
- Utilization in the CRC-1 of Kodak Technical Pan 2415 film, a very fine grain, black-and-white film providing the superior image resolution and contrast required for ultra precise applications.
- The development of AutoSet-1, also by Geodetic Services Inc., a fully automatic, computer controlled monocomparator with resolution of 0.1 μm and RMS repeatibility of 0.3 to 0.4 μm. Systematic errors of the scales are calibrated by means of a laser interferometer to an accuracy of 0.2 μm. Overall absolute accuracy, as established by calibration against a 150-point grid certified by the National Bureau of Standards, is 0.30 μm (RMS). AutoSet has automatic line following capabilities ideally suited to mensuration of images of plumb-lines.

With the CRC-1, in combination with AutoSet, systematic errors are suppressed to the extent that nonlinearity of plumb-line images is almost entirely attributable to distortion of the lens. Illustrations of the CRC-1 and AutoSet are provided in Figures 1 and 2, respectively.

With AutoSet the process of setting on images does not involve the exercise of human skill. Instead, this is accomplished automatically by means of digital image processing of a video scan. As a consequence, plumb-lines no longer need be very fine threads (0.3- to 0.4-mm diameter) in order to generate images optimized for human setting. In the tests described in this paper, lines of white translucent monofilament nylon cord of 1.25-mm (nominal) diameter were stretched reasonably vertically from ceiling to floor and maintained taut by means of turnbuckles. Measurements at several intervals showed RMS variability of cord diameter of 0.010 mm. Although the lines generated in this manner are not strictly plumb-lines, they shall be referred to as such for convenience. This is permissible because, in the version of the plumb-line cal-

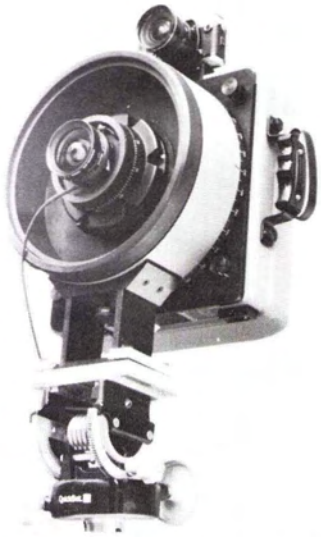

FIG.1. Close-Range Camera CRC-1 with 120-mm lens cone.

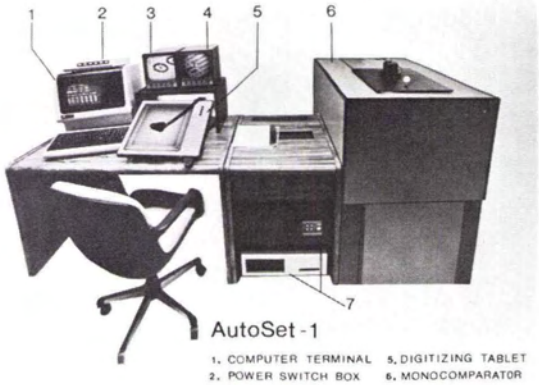

FIG.2. AutoSet-1.

ibration exercised, only linearity (and not parallelism) of the lines is assumed.

Twenty-five nominally vertical lines, each 3.0-m long and 150-mm apart, were set up in a plane just in front of a matte-black background. Lighting for the lines was provided by fluorescent light tubes placed around the periphery of the calibration range. The lighting was most intense at the edges, counteracting the natural fall-off of light toward the edge of the field of view of a lens, thereby producing an image having a uniform light distribution. Figure 3 shows the set up of the calibration range.

For a given focal setting of the lens, two exposures of Kodak Technical Pan film were made on

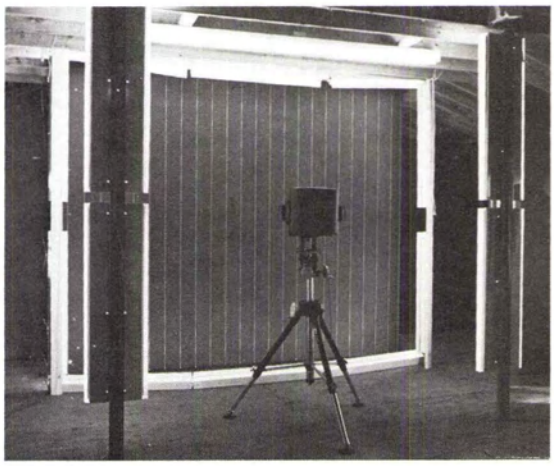

FIG.3. Plumb-line calibration range.

separate frames, the second with the camera rolled nominally 90° about its axis. Had both exposures been made on a common frame (as is more customary), plumb-line images would have formed a nearly orthogonal grid. In the present instance separate frames were used because intersections of grid lines could potentially interfere with the automatic line following operation of AutoSet. Exposure was generally two seconds at *f*/32. Photoprocessing was optimized for maximum contrast.

The initial phase of the monocomparator readings of the film consists of automatic searching and mensuration of the four fiducial and 25 reseau marks, the calibrated values of which reside in the AutoSet software. This operation takes less than 60 seconds to complete. A television monitor displays the process to the operator. False targets falling within the digitizing window of the monitor are usually automatically rejected by the image processing algorithm. However, on those relatively rare occasions when an unresolvable conflict exists, AutoSet simply proceeds to the next point, relegating the questionable point to a file for later recall and review by the operator. Such points can usually be salvaged by manipulation of the window to exclude false targets.

After the above process of initialization, the operator switches AutoSet to the line following mode. He then places the cursor on the beginning of a plumb-line image and requests a data point every, say, 4 mm. Thereupon, driving of the comparator stages and setting proceed automatically along the entire length of the line at a rate of one point per second.

Thirteen well spaced plumb-lines per photograph are usually followed in this manner, producing a data set of about 1300 points per pair of "horizontal" and "vertical" line traces. Total data gathering time of well under one hour is required for this automated procedure. This compares most favora-

bly with the five or so hours required for the 300-odd points manually observed with double settings on a Mann comparator as reported in the papers cited earlier (for example, Brown (1971), p. 862).

The diameter of the nylon monofilament was chosen to provide optimum images for the automatic target centering software of AutoSet. At a photographic scale of 1:10, a section of plumb-line approximately 180 micrometres long and 125 micrometres wide on the image is scanned to find the centroid. With an effective pixel size of 3.1 by 2.5 micrometres, about 3000 pixels are digitized. When such a large pixel population is available, the centroid of the target can be located to considerably better than a tenth of a pixel.

As the repeatability of the AutoSet monocomparator stage is 0.4 micrometres, the data being input to the distortion calculations is about five-fold more precise than that obtained by human setting. In the present investigation results are based on four times more data points than previously. This combined increase in precision and density of data serves to define more clearly the behavior of decentering distortion with varying object distance. It serves also to provide further and more precise validation of the model for variation of radial distortion with focusing.

RESULTS, RADIAL DISTORTION

The plumb-line range described in the preceding section was used to calibrate several camera/lens combinations in early 1985. The results of one of these calibrations is reproduced in Table 1 and illustrated in Figure 4. Particularly noteworthy in Table 1 are the low magnitudes of the RMS values of the x, y residuals of the measured coordinates. These are seen to range between 0.6 and 1.0 micrometres, with the larger values corresponding to the larger photographic scales. The explanation for this most likely lies in slight physical irregularities in the profile of the nylon cord which at a scale of 1:10 may amount to a sizable fraction of a micrometre.

To provide further verification of the exactness of Magill's (1955) formula as extended by Brown (1972) to account for the variation of radial distortion with focusing, the following calculation was performed and shown in Table 2. The observed values of radial distortion for scales of 1:10, 1:15, and 1:20 using a 240mm f/9 Fujinon-AS lens in camera CRC-010 are listed to a radial distance of 120 mm. The values for 1:15 scale are then compared to a set of values derived from the use of the 1:10 and 1:20 radial distortion coefficients using Equations 1 to 4 from Brown (1972). The discrepancies between the predicted and actually observed values are always less than 0.7 micrometres and the RMS value is 0.3 micrometres. Such results are consistent with the one-sigma error bounds of the distortion functions (these are under

TABLE 1. EXAMPLE OF RESULTS OF ANALYTICAL PLUMB-LINE CALIBRATIONS. STANDARD ERRORS IN PARENTHESES WERE EXTRACTED FROM COVARIANCE MATRIX OBTAINED FROM INVERSE OF NORMAL EQUATIONS. RMS ERRORS IN FINAL COLUMNS REFER TO RESIDUALS OF x,y MEASUREMENTS RESULTING FROM LEAST SQUARES ADJUSTMENT.

Camera: CRC-102 240-mm f/9 Fujinon-AS Lens.											
		Distortion Parameters (and Standard Errors)								RMS Errors (Micrometres)	
		Radial			Decentering						
Distance Camera-Plumb-Lines (metres)	Photo Scale	$K_1(10^{-7})$	$K_2(10^{-12})$	$K_3(10^{-18})$	$P_1(10^{-5})$	$P_2(10^{-5})$	$J_1(10^{-5})$	Φ_0 (deg.)		x	y
2.64	1:10	−0.662	0.467	0.554	−0.154	0.066	0.168	66.7		1.0	0.9
		(±0.007)	(±0.027)	(±0.134)	(±0.002)	(±0.002)	(±0.002)	(±0.5)			
3.84	1.15	−0.710	0.528	−0.544	−0.164	0.082	0.184	63.5		0.9	0.9
		(±0.009)	(±0.037)	(±0.133)	(±0.002)	(±0.002)	(±0.003)	(±0.7)			
5.04	1:20	−0.596	−0.636	−0.102	−0.158	0.108	0.191	55.5		0.6	0.7
		(±0.013)	(±0.083)	(±0.100)	(±0.003)	(±0.003)	(±0.004)	(±0.9)			

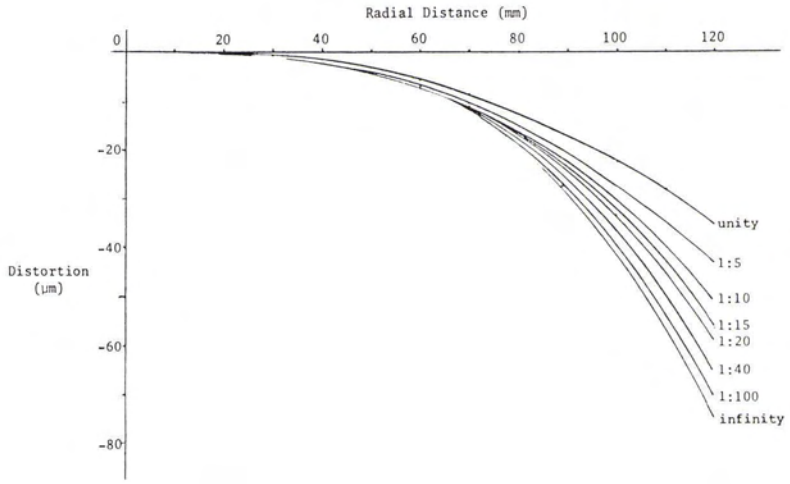

FIG.4. Gaussian radial distortion for varying photographic scales. Camera CRC-102, 240-mm *f*/9 Fujinon-AS lens. Values at 1:10, 1:15, and 1:20 determined from plumb-line calibration; other values computed from 1:10 and 1:20.

TABLE 2. VERIFICATION OF THE MODIFIED MAGILL (1955) FORMULA FOR THE VARIATION OF RADIAL DISTORTION WITH SCALE.

Camera: CRC-010 240-mm *f*/9 Fujinon-AS Lens.

Radial Distance	Observed Radial Distortion 1:10	1:15	1:20	Predicted 1:15 Radial Distortion Using 1:10 and 1:20	Difference Observed-Predicted
(1)	(2)	(3)	(4)	(5)	(3) – (5)
r mm	δr μm	δr μm	δr μm	δr μm	μm
20	−0.4	−0.4	−0.5	−0.4	0.0
40	−3.2	−3.4	−3.7	−3.5	+0.1
60	−10.5	−11.6	−12.5	−11.8	+0.2
80	−24.5	−27.4	−29.5	−27.7	+0.3
100	−46.9	−53.3	−57.3	−53.5	+0.2
120	−78.9	−91.8	−98.1	−91.1	−0.7

one micrometre and so are not separately presented).

RESULTS, DECENTERING DISTORTION

Brown (1966) produced the currently accepted form of the model for decentering distortion (see Equations 3 and 4) and used it over the following years to compute profiles of decentering distortion for a variety of cameras/lenses by means of stellar and plumb-line calibrations. Stellar calibrations obviously employed cameras focused at infinity, but one of the plumb-line calibrations indicated the possibility of decentering distortion varying with focusing (see Table 2 and Figure 5 in Brown (1971)). No firm conclusions could be drawn because of the uncertainty of the results and the limited sample of lenses.

After several camera/lens calibrations had been performed in 1985, the trend of decentering distortion varying with focusing was again observed, but this time the standard error of the tangential profile ($J_1 r^2$) was well below one micrometre. Consequently, a body of results emerged of sufficient sensitivity to define the behavior of decentering distortion with change in focus. This led to the development of the mathematical model presented below.

The phase angle of decentering distortion (ϕ_0) should be invariant with focusing. The actual variability found in Table 1 is higher than warranted by the standard errors of the individual determinations. Why this should be is unknown at present, but similar excessive variability of ϕ_0 has been found to be the rule more than the exception (for example, see Fritz and Schmid (1973)). However, no systematic variation in ϕ_0 with focusing has been observed.

EXTENSION TO ACCOUNT FOR VARIATION OF DECENTERING DISTORTION WITH OBJECT DISTANCE

A reexamination of the history of the decentering distortion showed that the thin prism model had been accepted by the photogrammetric community for 40 years (for example, Bennett (1927)) until Brown (1966) proved it to be projectively equivalent to the Conrady (1919) model. Explicit in the mathematical development of the thin prism distortion model is the principal distance '*c*', which is used as a scaling factor for the decentering distortion profile (see Equation 3, Brown (1966), p. 446). Upon conversion to the Conrady model (our Equations 3 and 4), there is no symbolic portrayal of the principal distance, *yet it is implicit to the definition of* J_1.

The use of Equations 3 and 4 for the calculation of the decentering distortion when the camera is not focused at infinity is not in strict conformance with the basic assumptions implicit in their derivation.

To clarify the situation, let the values of the decentering distortion that correspond to infinity focus (principal distance *c*) be designated as P_1, P_2, and J_1 and let c_s denote the principal distance corresponding to a focusing distance *s*. From the rigorous derivation of the thin prism model and its projective equivalence to the Conrady model, it follows that

$$P_{1s} = \frac{c}{c_s} P_1$$

$$P_{2s} = \frac{c}{c_s} P_2 \qquad (7)$$

$$J_{1s} = (P_{1s}^2 + P_{2s}^2)^{1/2} = \frac{c}{c_s} J_1$$

The principal distance c_s may be designated as $c + \Delta c_s$ where Δc_s is the focusing increment which by virtue of the thin lens formula is related to *c* and *s* by

$$\Delta c_s = \frac{c^2}{s-c}. \qquad (8)$$

This causes the expression $\frac{c}{c_s}$ in Equation 7 to reduce to

$$\frac{c}{c_s} = (1 - \frac{c}{s}). \qquad (9)$$

Transposition of Equations 7 permits coefficients of decentering distortion at infinity to be computed from those corresponding to the focusing distance *s*. The latter, of course, could be generated by means of a plumb-line calibration.

If the values of decentering distortion at infinity focus are to be chosen as the "standard" and designated as P_1, P_2, and J_1, it follows that the expressions for the decentering distortion Δx_s, Δy_s at an image point *x*, *y* can be represented more generally by

$$\Delta x_s = (1 - \frac{c}{s}) [P_1 (r^2 + 2x^2) + 2P_2 xy]$$

$$\Delta y_s = (1 - \frac{c}{s}) [P_2 (r^2 + 2y^2) + 2P_1 xy] \qquad (10)$$

where *s* is the distance on which the lens is focused. This result holds strictly only for points in the plane at *s*. As with symmetric radial distortion, a further modification is required to account for the variability within the photographic field. This is accomplished through application of the scaling factor $\gamma_{ss'}$ developed in Brown (1971) and defined as

$$\gamma_{ss'} = \frac{s - c}{s' - c} \frac{s'}{s} \qquad (11)$$

where *s* is, as above, the distance to the plane on which the camera is focused and *s'* is the distance to the plane of the point under consideration. To generate the formula for decentering distortion for a point at distance *s'* when the camera is focused at *s*, one must merely multiply the right hand sides of Equations 10 by the factor $\gamma_{ss'}$.

TABLE 3. OBSERVED DECENTERING DISTORTION PROFILES AT r = 100 MM FOR VARIOUS PHOTOGRAPHIC SCALES AND CORRESPONDING PREDICTED VALUES FOR INFINITY FOCUS.

Camera: CRC-102	120-mm *f*/8 Nikkor-SW Lens	
Photo Scale	Value $J_1 r^2$ r = 100 mm	Predicted Values $J_1 r^2$ at r = 100 mm (Infinity Focus)
1:8	28.9 μm	32.5 μm
1:12	29.6	32.1
1:16	29.7	31.6
1:20	31.0	32.5
Mean Infinity Value = 32.2 μm		
RMS = ±0.4		

EXPERIMENTAL CONFIRMATION

All the lenses tested in early 1985 were found to have decentering distortion profiles ($J_1 r^2$) which increase slowly in magnitude as the camera is moved further away from the plumb-lines, that is, $J_1 r^2$ increased as Δc_s (focusing) decreased. An example is shown in Table 3 for a 120-mm *f*/8 Nikkor-SW lens, measured at photographic scales of 1:8, 1:12, 1:16, and 1:20, respectively. The measured decentering profiles are shown in Figure 5.

The values of the decentering distortion profile for focus at infinity for a radial distance of 100 mm were predicted from each of these calibrations using Equation 7. Ideally, all should produce the same

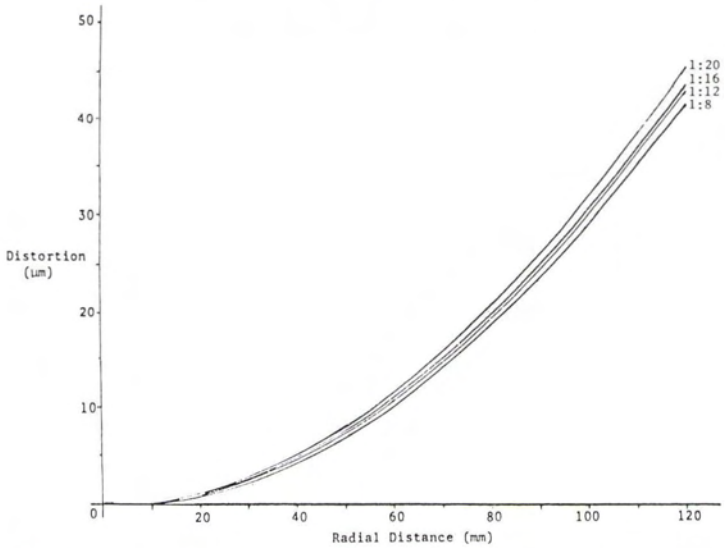

FIG.5. Observed decentering distortion profiles. Scales from 1:8 to 1:20, Camera CRC-102, 120-mm lens.

result. The mean value of 32.2 micrometres has a standard error of only 0.4 micrometres. Similar values, averaging 0.5 micrometres, were obtained from other camera calibrations. This not only provides good confirmation of the refined decentering model set forth in this paper but also serves as an indicator of the advances made by the combination of the CRC-1 and AutoSet.

PHOTOGRAMMETRIC IMPLICATIONS

The magnitude of the variation of decentering distortion within the photographic field is clearly dependent on the difference in the distances s and s'. As an example, consider the extreme case of a 240-mm lens focused for an object distance of 1 metre and an object in a plane 3 metres distant from the camera. If the decentering distortion profile were 30 µm for the focused plane, then for the distant point it would be 25 µm. More generally, however, the magnitude of this variation is likely to be quite small, often under 1 micrometre.

The fundamental correcting term $\gamma_{ss'}(1 - \frac{c}{s})$ equals unity at infinity focus, but for close range work can become quite significant. For example, if the profile of decentering distortion is 30 µm at a radial distance of 100 mm and P_1 and P_2 were calibrated at infinity, then at a photographic scale of 1:10 a 3-µm error will be made in the direction ϕ_0 of the maximum tangential distortion and up to 9 µm in the radial component of the decentering distortion in the direction $\phi_0 + 90°$.

While 30 micrometres of decentering distortion may seem large to users of aerial photogrammetric cameras, it is not uncommon for the types of lenses used in close-range applications.

The term $\gamma_{ss'}(1 - \frac{c}{s})$ is, of course, a scalar quantity. Consider the effect that this has on a bundle adjustment with self-calibration where P_1 and P_2 have been held invariant. If the same focal length setting had been used for all camera stations, assuming only one camera, then the P_1 and P_2 values returned from the self-calibration will be the best approximation for the decentering distortion at that focal length setting. The accuracy of the object coordinates will not have been degraded. If, on the other hand, several focal length settings were used, the results will be compromised because different decentering distortion values should have been computed for each focal length setting.

If the coefficient matrix for the decentering distortion terms P_1 and P_2 is modified by consideration of the term $\gamma_{ss'}(1 - \frac{c}{s})$, the process of self-calibration will provide values of P_1 and P_2 corresponding to infinity focus. This technique is recommended.

Another obvious implication concerns self-calibration over a finite range to produce parameters of lens distortion. If these values are used in subsequent applications without varying them according to the focal setting used, the results will be compromised.

CONCLUSIONS

Recent advances in technology have made the analytical plumb-line method a more powerful tool than ever before for lens calibrations. The development of the large format microprocessor-controlled CRC-

1 camera and the sub-micrometre precision of the automated monocomparator AutoSet enabled determinations of the decentering distortion profile to be made to an accuracy sufficient to uncover a shortcoming in the conventional formulae.

Decentering distortion was found to be a function of camera focusing. The generalized form of the model is given by Equations 10, modified when appropriate by the factor $\gamma_{ss'}$.

The new form of the model has been experimentally confirmed by a series of lens calibrations. Its adoption into algorithms for self-calibration is, therefore, recommended. The adoption of the infinity focus values as the "standard" for the terms P_1, P_2, J_1, and ϕ_0 is further recommended.

REFERENCES

Bennett, A., 1927. The Distortion of some Photographic Objectives, *Journal of the Optical Society of America*, Vol. 14, pp. 235–244.

Brown, D., 1966. Decentering Distortion of Lenses, *Photogrammetric Engineering*, Vol. 32, No. 3., pp. 444–462.

———, 1971. Close-Range Camera Calibration, *Photogrammetric Engineering*, Vol. 37, No. 8, pp. 855–866.

———, 1972. Calibration of Close Range Cameras, Invited Paper, XII Congress of ISP, Ottawa, Canada Commission V, 25 p.

———, 1984. A Large Format Microprocessor Controlled Film Camera Optimized for Industrial Photogrammetry, Presented Paper, XV Congress of ISP, Rio de Janeiro, 28 p.

Conrady, A., 1919. Decentered Lens Systems, *Monthly Notices of the Royal Astronomical Society*, Vol. 79, pp. 384–390.

Fritz, L., and H. Schmid, 1973. An Operational Camera Calibration by the Stellar Method at NOAA/NOS, *Proc. A.S.P. Fall Convention*, Florida, pp. 285–307.

Magill, A., 1955. Variation in Distortion with Magnification, *Journal of Research of the National Bureau of Standards*, Vol. 54, No. 3, pp. 135–142, Research Paper 2574.

(Received 1 April 1985; accepted 24 May 1985; revised 4 September 1985)

CALL FOR PAPERS

IAPR TC 7 Workshop on Analytical Methods in Remote Sensing for Geographic Information Systems

IBM Scientific Center, Paris
23-24 October 1986

The IAPR TC 7 workshop is being organized by the Technical Committee 7 (Application in Remote Sensing) of the International Association of Pattern Recognition and sponsored by the IBM Scientific Center in Paris. The purpose of the workshop is to provide a forum for scientists to share their recent findings in the following areas:

- Analytical Methods in Remote Sensing
- The Processing of Multi-Source Data
- The Integration of Remote Sensing Data in Geographic Information Systems
- The Role of Artificial Intelligence in Remote Sensing

The workshop is organized into four sessions, each starting with an invited talk followed by selected presentations and discussions. Prospective participants are invited to submit an abstract of about 400 words on their original research before *28 February 1986* to:

Dr. P. T. Nguyen
IBM Scientific Center
36 ave Raymond Poincare
75116 Paris, France
Tele. (1) 505 14 00 ext. 2822